

Carbene Formation in Its Lower Singlet State from Photoexcited 3*H*-Diazirine or Diazomethane. A Combined CASPT2 and *ab Initio* Direct Dynamics Trajectory Study

Juan F. Arenas,* Isabel López-Tocón, Juan C. Otero, and Juan Soto

Contribution from the Department of Physical Chemistry, Faculty of Sciences, University of Málaga, E-29071 Málaga, Spain

Received March 21, 2001. Revised Manuscript Received July 17, 2001

Abstract: The potential energy surfaces of the ground and valence excited states of both 3*H*-diazirine and diazomethane have been studied computationally by mean of the CASSCF method in conjunction with the cc-pVTZ basis set. The energies of the critical points found on such surfaces have been recomputed at the CASPT2/cc-pVTZ level. Additionally, *ab initio* direct dynamic trajectory calculations have been carried out on the S₁ and S₂ surfaces, starting each trajectory run at the region dominated by the conformational molecular rearrangement of diazomethane. It is found that both isomers are interconnected along a C_s reaction coordinate on each potential surface. Radiationless deactivation of the corresponding S₁ state of each isomer occurs through the same point on the surface, an S₁/S₀ conical intersection. Thereafter, the system has enough energy to surmount the barrier which leads to dissociation products (CH₂ + N₂) on S₀ state. Therefore, photoexcitation to S₁ state of either diazirine or diazomethane produces methylene in its lower singlet state on a very short time scale (ca. 100 fs). Furthermore, both isomers can generate excited singlet carbene when they are excited onto the S₂ surface; in this case, they lose the activation energy passing through another common S₂/S₁ conical intersection and then proceed to dissociation into carbene and N₂ on the S₁ surface. For the special case of methylene, it rapidly experiences deexcitation to S₀ state.

Introduction

Carbenes, as reactive intermediates, occupy a significant place in all branches of chemistry.¹ Among the methods used for the generation of such intermediates are the photolysis and thermolysis of diazirine and diazo compounds. Diazirines are preferred precursors compared to acyclic diazo compounds because of their stability and ease of handling.² In principle, diazirines and diazo compounds can undergo two important photoreactions: (1) nitrogen extrusion to give the corresponding carbene; (2) diazirine \rightleftharpoons diazo isomerization. While the formation of diazo compounds as intermediates during the photolysis of diazirines is unquestioned,³ their existence on photolysis of 3*H*-diazirine itself, the family parent, has been controversial.² Amrich and Bell⁴ identified diazomethane as a reaction product in the gas photolysis of mixtures of 3*H*-diazirine and molecular nitrogen, which was interpreted as a proof of photoisomerization of diazirine.

On the other hand, the experiments of Moore and Pimentel⁵ do not agree with those of the former authors. They concluded from isotopic labeling experiments that the photolysis of either

diazomethane or diazirine isolated in solid nitrogen matrix produces methylene (CH₂) molecules, which subsequently recombine with N₂ to form diazomethane. However, no diazomethane was detected in the gas photolysis of diazirine-*d*₂.

Two other questions to address are (1) the electronic state in which methylene is formed and (2) the first reaction step after light excitation. It was experimentally found that the distributions of isomers formed on pyrolysis and photolysis of diazirines are very different.⁶ To explain these observations, it was postulated that a single intermediate could not be common to both thermal and photochemical processes. Consequently, it was proposed that photolysis of the diazirines might yield the carbenes in their excited states from which the distinct isomers were generated.⁶ Another point of view was first given by Frey^{7a} and later by Platz and co-workers.^{7b-g} These authors lend support to the hypothesis that a most economical interpretation of the product studies could be the rearrangement in the excited state of the diazirine (the RIES mechanism), the formation of the excited

* Address correspondence to this author.

(1) Dürr, H.; Abdel-Wahab, A.-M. In *A CRC Handbook of Organic Photochemistry and Photobiology*; CRC Press: Boca Raton, FL, 1995; p 960.
(2) Liu, M. T. *Chem. Soc. Rev.* **1981**, *11*, 127.
(3) (a) Bonneau, R.; Liu, M. T. *J. Am. Chem. Soc.* **1996**, *118*, 7229. (b) Seburg, R. A.; McMahon, R. J. *J. Am. Chem. Soc.* **1992**, *114*, 7183. (c) Frey, H. M. *Adv. Photochem.* **1966**, *4*, 225.
(4) Amrich, M. J.; Bell, J. A. *J. Am. Chem. Soc.* **1964**, *86*, 292.
(5) Moore, C. B.; Pimentel, G. C. *J. Chem. Phys.* **1964**, *41*, 3504.

(6) (a) Mansoor, A. M.; Stevens, I. D. R. *Tetrahedron Lett.* **1966**, 1733. (b) Chang, K. T.; Shechter, H. *J. Am. Chem. Soc.* **1979**, *101*, 5082. (d) Figuera, J. M.; Pérez, J. M.; Tobar, A. *J. Chem. Soc., Faraday Trans. 1* **1978**, *74*, 809.
(7) (a) Frey, H. M.; Stevens, I. D. R. *J. Chem. Soc.* **1965**, 1700. (b) Modarelli, D. A.; Platz, M. S. *J. Am. Chem. Soc.* **1991**, *113*, 8985. (c) Modarelli, D. A.; Morgan, S.; Platz, M. S. *J. Am. Chem. Soc.* **1992**, *114*, 7034. (d) White, W. R., III.; Platz, M. S. *J. Org. Chem.* **1992**, *57*, 2841. (e) Modarelli, D. A.; Platz, M. S. *J. Am. Chem. Soc.* **1993**, *115*, 470. (f) Buterbaugh, J. S.; Toscano, J. P.; Weaver, W. L.; Gord, J. R.; Hadad, C. M.; Gustafson, T. L.; Platz, M. S. *J. Am. Chem. Soc.* **1997**, *119*, 3580. (g) Ford, F.; Yuzawa, T.; Platz, M. S.; Matzinger, S.; Fülischer, M. *J. Am. Chem. Soc.* **1998**, *120*, 4430.

carbene being another reaction path. The observations made by other research groups⁸ also supported the RIES mechanism, with variable efficiency with respect to the carbene route. Finally, it cannot be discarded a priori that the differences of the product distributions arise from a common intermediate (carbene in its lower singlet state) subject to dynamical effects; for a recent review on this subject see Carpenter.¹⁰ This point of view agrees with the most recent studies done on the photoreaction of methyl α -diazo-(2-naphthyl)acetate,⁹ which show that the product of the Wolff rearrangement of such a compound, ketene, is formed predominantly from the spin-equilibrated carbene rather than from a diazo excited state.

In this work, we report our findings in studying the topological features of the potential energy surfaces involved in the photochemical and thermal reactions of 3H-diazirine and diazomethane. Several theoretical works on the photochemistry of diazirine derivatives have been carried out by other groups and ourselves;^{11–14} however, some new vistas are achieved when a refined treatment is applied to both systems (see Computational Details). For example, the most striking conclusion of this paper is that methylene is generated in its lowest singlet state, after radiationless electronic deexcitation of its precursor, either diazirine or diazomethane. The extent to which 3H-diazirine's photochemistry resembles more complex systems is not clear only from this study. However, it must be pointed out that the decay pathways must be quite similar for related species, although, of course, there are enough differences between two different molecules to anticipate that the intramolecular vibrational redistribution (IVR) in the excited state must play a key role, leading to unequal partitioning among the possible routes. Thus, in accordance with Carpenter's belief, we think that dynamic effects and not the shapes of the potential energy surfaces will change the behaviors of two related molecules. Therefore, the parents of the diazirine and diazo families should be good models for understanding the photochemistry of such compounds, at least the alkyl family.

In discussing the potential energy surfaces, we will use both photochemical and spectroscopic conventions to label such surfaces; by way of introduction, the relevant orbitals in the photochemistry of both isomers, diazirine and diazomethane, are shown in Figure 1. In turn, these orbitals have been used in the definition of the active space.

Computational Details

The geometries of all stationary points relevant to the thermal and photochemical reactions of 3H-diazirine and diazomethane have been optimized with the CASSCF approximation¹⁵ as implemented in the

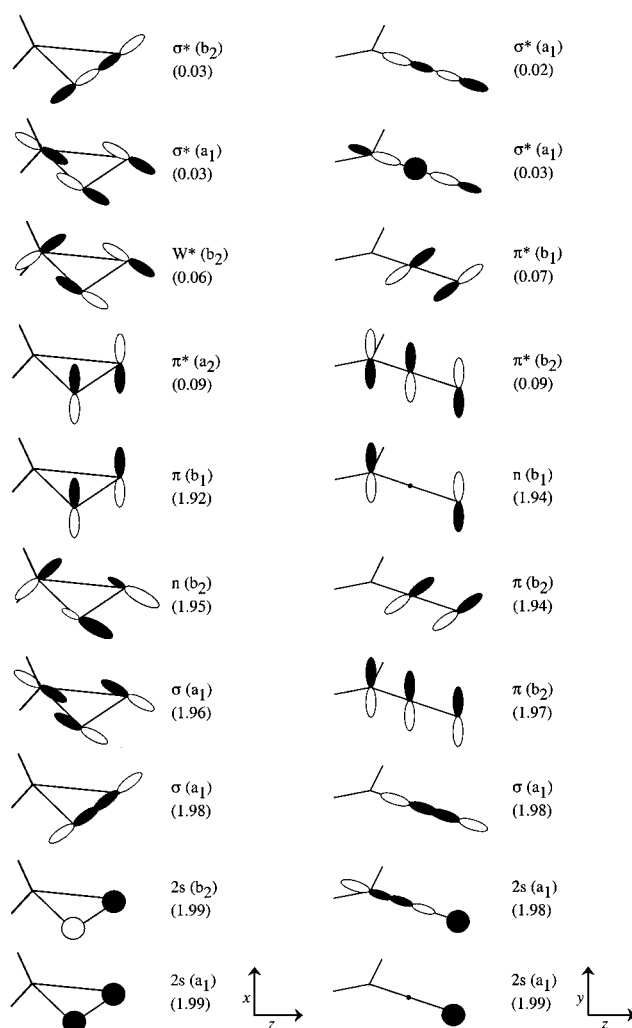


Figure 1. Schematic plot of the molecular orbitals included in the definitions of the active spaces of diazirine and diazomethane.

package of programs MOLCAS 5.0.¹⁶ Dunning's correlation-consistent polarized valence triple- ζ basis set (cc-pVTZ)¹⁷ has been used throughout this work.

The localization and optimization of the lower energy points in the seam of crossing between two states of the same spin multiplicity, conical intersections (CI), which are involved in internal conversion processes, have been performed at the CASSCF level as well, by using the algorithm¹⁸ implemented in the MC-SCF code released in GAUSSIAN 98.¹⁹ In the seam of crossing of two surfaces, the energy is minimized along a $(3N - 8)$ -dimensional hyperline, N being the number

- (8) (a) La Villa, J. A.; Goodman, J. L. *Tetrahedron Lett.* **1990**, *31*, 5109. (b) Moss, R. A.; Liu, W. J. *J. Chem. Soc., Chem. Commun.* **1993**, 1597. (c) Bonneau, R.; Liu, M. T. H.; Kim, K. C.; Goodman, J. L. *J. Am. Chem. Soc.* **1996**, *118*, 3829.
- (9) (a) Zhu, Z.; Bally, T. Stracener, L. L.; McMahon, R. J. *J. Am. Chem. Soc.* **1999**, *121*, 2863. (b) Wang, Y.; Yuzawa, T.; Hamaguchi, H.; Toscano, J. P. *J. Am. Chem. Soc.* **1999**, *121*, 2875. (c) Wang, J.-L.; Likhovorik, I.; Platz, M. S. *J. Am. Chem. Soc.* **1999**, *121*, 2883.
- (10) Carpenter, B. K. *Angew. Chem., Int. Ed.* **1998**, *37*, 3340.
- (11) Bernardi, F.; Olivucci, M.; Robb, M. A.; Vreven, T.; Soto, J. *J. Org. Chem.* **2000**, *65*, 7847.
- (12) Yamamoto, N.; Bernardi, F.; Bottoni, A.; Olivucci, M.; Robb, M. A.; Wilsey, S. J. *J. Am. Chem. Soc.* **1994**, *116*, 2064.
- (13) Müller-Remmers, P. L.; Jug, K. *J. Am. Chem. Soc.* **1985**, *107*, 7275.
- (14) Bigot, B.; Poncet, R.; Sevin, A.; Devaquet, A. *J. Am. Chem. Soc.* **1978**, *100*, 6575.
- (15) Roos, B. O. In *Advances in Chemical Physics; Ab Initio Methods in Quantum Chemistry—II*; Lawley, K. P., Ed.; John Wiley & Sons: Chichester, England, 1987; Chapter 69, p 399.

- (16) Andersson, K.; Barysz, M.; Bernhardsson, A.; Blomberg, M. R. A.; Cooper, D. L.; Fleig, T.; Fülischer, M. P.; de Graaf, C.; Hess, B. A.; Karlström, G.; Lindh, R.; Malmqvist, P.; Neogrády, P.; Olsen, J.; Roos, B. O.; Sadlej, A. J.; Schütz, M.; Schimmelpfennig, B.; Seijo, L.; Serrano-Andrés, L.; Siegbahn, P.; Ståhring, J.; Thorsteinsson, T.; Veryazov, V.; Widmark, P. *MOLCAS Version 5*; Lund University: Sweden, 2000.
- (17) Dunning, T. H., Jr. *J. Chem. Phys.* **1989**, *90*, 1007.
- (18) Ragazos, I. N.; Robb, M. A.; Bernardi, F.; Olivucci, M. *Chem. Phys. Lett.* **1992**, *197*, 217.
- (19) Frisch, M. J.; Trucks, G. W.; Schlegel, H. B.; Scuseria, G. E.; Robb, M. A.; Cheeseman, J. R.; Zakrzewski, V. G.; Montgomery, J. A., Jr.; Stratmann, R. E.; Burant, J. C.; Dapprich, S.; Millam, J. M.; Daniels, A. D.; Kudin, K. N.; Strain, M. C.; Farkas, O.; Tomasi, J.; Barone, V.; Cossi, M.; Cammi, R.; Mennucci, B.; Pomelli, C.; Adamo, C.; Clifford, S.; Ochterski, J.; Petersson, G. A.; Ayala, P. Y.; Cui, Q.; Morokuma, K.; Malick, D. K.; Rabuck, A. D.; Raghavachari, K.; Foresman, J. B.; Cioslowski, J.; Ortiz, J. V.; Stefanov, B. B.; Liu, G.; Liashenko, A.; Piskorz, P.; Komaromi, I.; Gomperts, R.; Martin, R. L.; Fox, D. J.; Keith, T.; Al-Laham, M. A.; Peng, C. Y.; Nanayakkara, A.; Gonzalez, C.; Challacombe, M.; Gill, P. M. W.; Johnson, B. G.; Chen, W.; Wong, M. W.; Andres, J. L.; Head-Gordon, M.; Replogle, E. S.; Pople, J. A. *Gaussian 98*, revision A.7; Gaussian, Inc.: Pittsburgh, PA, 1998.

of atoms in the molecule. Davidson²⁰ has demonstrated for the polyatomic case that there are two directions, namely x_1 (gradient difference) and x_2 (nonadiabatic coupling), which lift the degeneracy of the states as one distorts the molecular geometry from the conical intersection point. All of the computations of the crossing surfaces have been performed with state-average orbitals,²¹ which ensure a balanced description at the intersection geometries without imposing symmetry on the wave function and avoiding symmetry breaking.²²

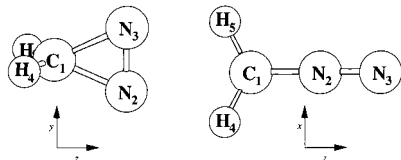
On the basis of the optimized geometries, the energies of all critical points have been recomputed with the CASPT2 method.²³ Therefore, the CASSCF wave functions were used as reference in the second-order perturbation treatment, keeping frozen the 1s electrons of the carbon and nitrogen atoms respectively, as determined in the SCF calculations.

The molecular orbitals chosen for the active space were those arising from all “valence” orbitals of the chromophore ($-\text{CN}_2$), that is, 12 electrons distributed in 10 orbitals, hereafter designated (12e, 10o). Formally, these orbitals represent in the S_0 minimum of diazirine one $\pi(\text{N}-\text{N})$, one $\pi^*(\text{N}-\text{N})$, one $\sigma(\text{N}-\text{N})$, $\sigma^*(\text{N}-\text{N})$, two $\sigma(\text{C}-\text{N})$, and two $\sigma^*(\text{C}-\text{N})$ bonds, plus the 2s atomic orbitals of the nitrogen atoms, respectively. One of the $\sigma(\text{C}-\text{N})-\sigma^*(\text{C}-\text{N})$ bond pairs transforms to a $\pi(\text{N}-\text{N})-\pi^*(\text{N}-\text{N})$ pair in diazomethane; the acyclic isomer.

The stationary points (minima and saddle points) have been characterized by their CASSCF/cc-pVTZ analytic harmonic vibrational frequencies computed by diagonalizing the mass-weighted Cartesian force constant matrix, i.e., the Hessian matrix \mathbf{H} . In turn, these frequencies have been used for the zero-point-energy (ZPE) corrections. The frequencies for ZPE corrections to the conical intersection points have been calculated in a different manner by calculating the projected Hessian matrix²⁴ \mathbf{H}^p .

Additionally, ab initio direct²⁵ semiclassical trajectory calculations in the full space of coordinates with surface hopping²⁶ have been performed with a reduced active space²⁷ CASSCF(8,7) in conjunction with the 6-31G* basis set.²⁸ In this approach, the electrons are treated quantum mechanically and the nuclei classically. Furthermore, it is not necessary to compute previously the potential energy surface but the gradient, energy, and frequencies are calculated at each step of the trajectory run without imposing any geometric restriction. However, the energy gradient and Hessian have to be computed at each point in the dynamic study. Given that the CASSCF calculation is an expensive method for such a purpose, only a few representative trajectories can be run in practice. The algorithm for trajectory surface hop of Tully and Preston²⁶ is used to propagate excited state trajectories onto the

Table 1. Geometrical Parameters for the Stationary Points (in C_{2v} Symmetry) on the Ground and Low-Lying Excited Potential Energy Surfaces of Diazirine (DZ) and Diazomethane (DM)^{a,b}



| | C_1-N_2 | N_2-N_3 | C_1-H_4 | $C_5-N_2-N_3$ | $H_4-C_1-H_5$ |
|-------------------------------|-----------|-----------|-----------|---------------|---------------|
| experimental ^c DZ | 1.482 | 1.228 | 1.09 | 65.5 | 117 |
| A_1 , ground state DZ | 1.500 | 1.237 | 1.069 | 65.7 | 120.3 |
| B_1 , 1st excited state DZ | 1.613 | 1.263 | 1.066 | 67.0 | 123.4 |
| B_2 , 2nd excited state DZ | 1.413 | 1.657 | 1.096 | 54.1 | 110.7 |
| A_2 , 3rd excited state DZ | 1.483 | 1.464 | 1.076 | 60.4 | 117.6 |
| experimental ^d DM | 1.32 | 1.12 | 1.08 | 180 | 127 |
| A_1 , ground state DM | 1.320 | 1.140 | 1.065 | 180 | 126.1 |
| A_2 , 1st excited state DM | 1.366 | 1.202 | 1.072 | 180 | 121.9 |
| $2A_1$, 2nd excited state DM | 1.741 | 1.174 | 1.059 | 180 | 139.8 |
| B_2 , 3rd excited state DM | 1.403 | 1.115 | 1.227 | 180 | 164.3 |
| $2A_2$, 4th excited state DM | 1.373 | 1.371 | 1.072 | 180 | 121.6 |

^a Evaluated at the CASSCF/cc-pVTZ level. ^b Internuclear distances are given in angstroms and bond angles in degrees. ^c From ref 31; the structural parameters d_{CN} and d_{NN} are the so-called r_s parameters since they were obtained by using only isotopic shifts in the moments of inertia. ^d From ref 32; only the sum $d_{\text{CN}} + d_{\text{NN}} = 2.442$ is accurately known.

ground-state surface in the region of a conical intersection. As demonstrated analytically by Herman²⁹ and suggested by many other authors,³⁰ after a surface hop, the energy difference between the two electronic states is redistributed along the momentum parallel to the nonadiabatic coupling vector. The probability of a surface hop, a_{ij}^2 , is determined from two coupled differential equations:

$$i\hbar\dot{a}_{ij} = \sum_l \{a_{lj}[\langle\phi_k|H|\phi_l\rangle - i\hbar\dot{\mathbf{R}}\mathbf{d}_{kl}] - a_{kl}[\langle\phi_l|H|\phi_j\rangle - i\hbar\dot{\mathbf{R}}\mathbf{d}_{lj}]\} \quad (1)$$

where ϕ_k are zero-order wave functions, $\langle\phi_k|H|\phi_l\rangle$ are CI-Hamiltonian matrix elements, $\dot{\mathbf{R}}$ is the nuclear velocity, and \mathbf{d}_{kl} is the nonadiabatic coupling vector. The term responsible for coupling the two (adiabatic) states is the nuclear velocity multiplied by the nonadiabatic coupling vector; that is, only those trajectories “orthogonal” to the seam of crossing and with enough velocity will be effective to induce a surface hop.

Results and Discussion

Both diazirine and diazomethane ground states possess C_{2v} symmetry. Three and four valence excited states arise from these two species, respectively. Each of these valence states gives a C_{2v} stationary point on the corresponding potential energy surface. The geometric parameters of such points along with their electronic symmetries are collected in Table 1 and their energies in Table 2. By comparison of the agreement between the experimental and calculated magnitudes, one can check the reliability of the calculations.

Ground-State Potential Energy Surface. The calculated equilibrium geometries of both isomers, diazirine and diazomethane, agree very well with the experimental parameters.^{31,32} Two reaction paths are found on the potential energy surface of the ground state, S_0 : (1) isomerization of diazirine to diazomethane; (2) decomposition of diazirine to give singlet

- (20) Davidson, E. R. *J. Am. Chem. Soc.* **1977**, *99*, 397.
 (21) (a) Werner, H.; Meyer, W. *J. Chem. Phys.* **1981**, *74*, 5794. (b) Hinze, J. *J. Chem. Phys.* **1973**, *59*, 6424. (c) Lengsfeld, B. H. *J. Chem. Phys.* **1982**, *77*, 4073. (d) Diffenderfer, R. N.; Yarkony, D. R. *J. Phys. Chem.* **1982**, *86*, 5098.
 (22) Frey, R. F.; Davidson, E. R. In *Advances in Molecular Electronic Structure Theory: Calculation and Characterization of Potential Energy Surfaces*; Wiley: New York, 1990; Vol. 1.
 (23) (a) Andersson, K.; Malmqvist, P.-Å.; Roos, B. O.; Sadlej, A. J.; Wolinski, K. *J. Phys. Chem.* **1990**, *94*, 5483. (b) Andersson, K.; Malmqvist, P.-Å.; Roos, B. O. *J. Chem. Phys.* **1992**, *96*, 1218. (c) Andersson, K.; Roos, B. O. In *Advances Series in Physical Chemistry; Modern Electron Structure Theory*; Yarkony, D. R., Ed.; World Scientific: Singapore, 1995; Vol. 2, part I, p 55.
 (24) (a) Miller, W. H.; Handy, N. C.; Adams, J. E. *J. Chem. Phys.* **1980**, *72*, 99. (b) Arenas, J. F.; Marcos, J. I.; López-Tocón, I.; Otero, J. C.; Soto, J. *J. Chem. Phys.* **2000**, *113*, 2282. (c) Arenas, J. F.; Marcos, J. I.; Otero, J. C.; Tocón, I. L.; Soto, J. *Int. J. Quantum Chem.* **2001**, *84*, 241.
 (25) (a) Helgaker, T.; Uggerud, E.; Jensen, H. *J. Am. Chem. Phys. Lett.* **1990**, *173*, 145. (b) Helgaker, T.; Uggerud, E. *J. Am. Chem. Soc.* **1992**, *114*, 4265.
 (26) (a) Tully, J. C.; Preston, R. K. *J. Chem. Phys.* **1971**, *55*, 562. (b) Tully, J. C. *J. Chem. Phys.* **1990**, *93*, 1061.
 (27) It is found that the minimal active space, which properly describes the topological feature of the potential surfaces of the region of diazomethane, comprises eight electrons distributed in seven orbitals. The orbitals which are not included with respect to the larger active space (12e, 10o) are the 2s and $\sigma^*(\text{N}-\text{N})$ ones. See Supporting Information for further details.
 (28) (a) Ditchfield, R.; Hehre, W. J.; Pople, J. A. *J. Chem. Phys.* **1971**, *54*, 724. (b) Hehre, W. J.; Ditchfield, R.; Pople, J. A. *J. Chem. Phys.* **1972**, *56*, 2257. (c) Hariharan, P. C.; Pople, J. A. *Theor. Chim. Acta* **1973**, *28*, 213.

- (29) Herman, M. F. *J. Chem. Phys.* **1984**, *81*, 754.
 (30) (a) Blais, N. C.; Truhlar, D. G.; Mead, C. A. *J. Chem. Phys.* **1988**, *89*, 6204. (b) Stine, J. R.; Muckerman, J. C. *J. Phys. Chem.* **1987**, *91*, 459.
 (31) Pierce, L.; Dobyns, V. *J. Am. Chem. Soc.* **1962**, *84*, 2651.
 (32) Cox, A. P.; Thomas, L. F.; Sheridan, J. *Nature (London)* **1958**, *181*, 1000.

Table 2. Energetic of the Critical Points on the Potential Energy Surfaces of Diazirine (DZ) and Diazomethane (DM)

| description | CASSCF ^a | CASPT2 ^a | weight ^b | T_0^c | T_0^d | expt ^e |
|--------------------|---------------------|---------------------|---------------------|------------------|------------------|--------------------|
| A ₁ DZ | -148.053 65 | -148.447 49 | 0.904 | 0.0 ^f | 0.0 ^f | 0.0 ^f |
| B ₁ DZ | -147.889 29 | -148.305 85 | 0.891 | 322 ^f | 323 ^f | 325 ^j |
| B ₂ DZ | -147.773 01 | -148.227 31 | 0.860 | 207 ^f | 207 ^f | 200 ^k |
| A ₂ DZ | -147.797 54 | -148.219 69 | 0.888 | 200 ^f | 200 ^f | 200 ^k |
| A ₁ DM | -148.073 26 | -148.463 12 | 0.903 | 0.0 ^g | 0.0 ^g | 0.0 ^g |
| A ₂ DM | -147.956 14 | -148.363 97 | 0.893 | 460 ^g | 461 ^g | 471 ^{g,m} |
| 2A ₁ DM | -147.847 31 | -148.253 18 | 0.883 | 217 ^g | 217 ^g | 218 ^{g,m} |
| 2A ₂ DM | -147.789 68 | -148.212 71 | 0.879 | 182 ^g | 182 ^g | 190 ^{g,m} |
| B ₂ DM | -147.826 31 | -148.238 11 | 0.880 | 202 ^g | 204 ^g | |
| TS0 | -147.982 48 | -148.380 24 | 0.896 | 677 ^h | 683 ⁱ | |
| TS1 | -148.015 73 | -148.398 43 | 0.902 | 929 ^h | 937 ⁱ | |
| TS2 | -147.739 33 | -148.180 35 | 0.865 | 171 ^h | 171 ⁱ | |
| CII | -147.949 63 | -148.39688 | 0.881 | 900 ^h | 909 ⁱ | |
| CI2 | -147.887 59 | -148.298 23 | 0.891 | 305 ^h | 306 ⁱ | |

^a Energy in hartrees. ^b Weight of the reference wave function. ^c Origin of the band system in nm. ^d 0–0 transition in nm. ^e Observed transitions in nm. ^f Transition energy in nm with respect to S₀ diazirine. ^g Transition energy in nm with respect to S₀ diazomethane. ^h Must be read as relative energy to A₁ DZ without ZPE correction. ⁱ Must be read as relative energy to A₁ DZ with ZPE correction. ^j Reference 35. ^k Reference 39. ^m Reference 36.

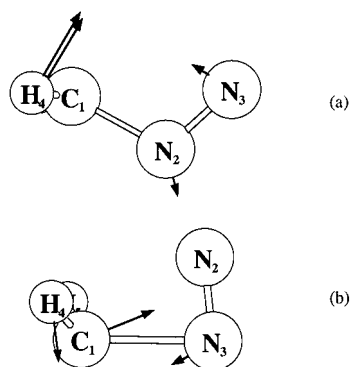


Figure 2. Optimized structures on the ground-state surface at the CASSCF-(12,10)/cc-pVTZ level: (a) TS0 transition state for diazirine \rightleftharpoons diazomethane isomerization; (b) TS1 transition state for N₂ extrusion from diazirine. The arrows on the plotted structures correspond to the transition vectors.

carbene and molecular nitrogen. These paths lie essentially in a C_s symmetry reaction coordinate. The structures of the transition states for both channels are plotted in Figure 2, and their energies are collected in Table 2. The calculated reaction energy (9.9 kcal/mol) compares very well with the experimentally determined value (8 ± 5 kcal/mol)³³ for isomerization from diazirine to diazomethane, which is a further probe to check the reliability of the CASPT2 calculations. The minima connected by each transition state were unambiguously determined by performing the corresponding IRC calculations.³⁴ It is clear from the computed barrier energy heights (Table 2) that methylene formation is a favored process with respect to isomerization.

First-Excited-State Potential Energy Surface. The first excited state is the most important one to be considered, given that most of the experimental work done on the photochemistry of diazirine and diazo derivatives start on this state.

On the S₁ potential energy surface, we have localized two stationary points with C_{2v} symmetry corresponding to the excited

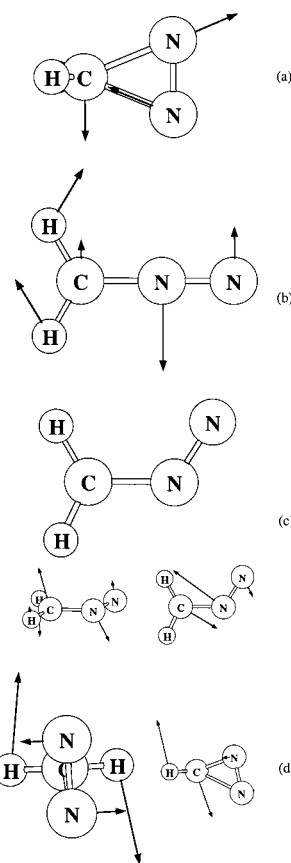


Figure 3. Critical points on the S₁ surfaces: (a) first-order saddle point corresponding to the stationary structure of diazirine; (b) first-order saddle point corresponding to the stationary structure of diazomethane; (c) CII S₁/S₀ conical intersection for diazirine \leftrightarrow diazomethane “isomerization”, the structures at the bottom of the figure correspond to the nonadiabatic coupling (left) and gradient difference (right) vectors; (d) two perspectives of the bifurcation point.

states of diazirine and diazomethane (Table 1). The computed 0–0 transition wavelengths are 323 and 461 nm, respectively, in agreement with the experimental values^{35,36} (325, 471 nm). The first excited state of either diazirine or diazomethane corresponds to an n–π* excitation. However, both states belong to different symmetry species, B₁ in diazirine and A₂ in diazomethane, in accordance with our Cartesian reference system (Table 1). They are not local minima at all but are saddle points on the S₁ excited-state surface. The normal coordinates corresponding to the imaginary modes of such points are plotted in parts a and b, respectively, of Figure 3. It is clear from Figure 3a that motion along this normal coordinate leads from S₁ diazirine to S₁ diazomethane.

On the other hand, an IRC calculation ends at an S₁/S₀ conical intersection (CII, Figure 3c) which represents the global “minimum” of the S₁ n–π* excited-state surface. At such a point, an efficient radiationless decay from S₁ to S₀ states occurs.

Therefore, there are two saddle points connected along a C_s symmetry coordinate. As mentioned by Castaño et al.,³⁷ it can be mathematically demonstrated that a valley–ridge inflection (VRI) point or bifurcation³⁸ must exist along the minimum energy path (MEP).

(33) Benson, S. W.; Cruickshank, F. R.; Golden, D. M.; Haugen, G. R.; O’Neal, H. E.; Rodgers, A. S.; Shaw, R.; Walsh, R. *Chem. Rev.* **1969**, *69*, 279.

(34) (a) González, C.; Schlegel, H. B. *J. Chem. Phys.* **1989**, *90*, 2154. (b) González, C.; Schlegel, H. B. *J. Phys. Chem.* **1990**, *94*, 5523.

(35) Graham, W. H. *J. Am. Chem. Soc.* **1962**, *84*, 1063.

(36) Herzberg, G. In *Molecular Spectra and Molecular Structure. III. Electronic Spectra and Electronic Structure of Polyatomic Molecules*; Van Nostrand: New York, 1966; p 623.

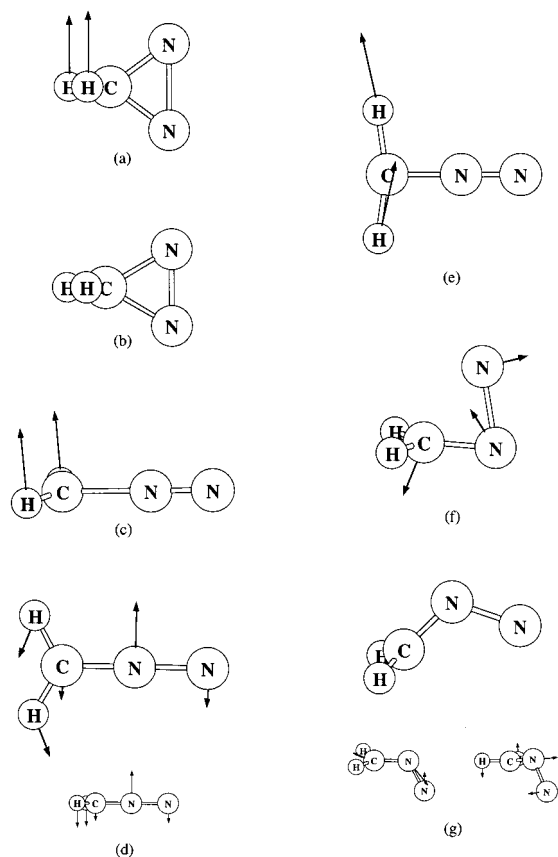


Figure 4. Critical points on the S_2 and S_3 surfaces: (a) first-order saddle point corresponding to the S_2 stationary structure of diazirine; (b) S_3 minimum of diazirine; (c) first-order saddle point corresponding to the S_2 stationary structure of diazomethane; (d) second-order saddle point corresponding to the S_3 stationary structure of diazomethane, the structure at the bottom of the figure shows the second imaginary transition vector; (e) first-order saddle point corresponding to the S_4 stationary structure of diazomethane; (f) TS2 transition state for ring opening of diazirine on the S_2 surface; (g) CI2 S_2/S_1 conical intersection, the structures at the bottom of the figure correspond to the nonadiabatic coupling (left) and gradient difference (right) vectors.

To localize the bifurcation point, we have calculated the analytical frequencies at each interpolation step of the approximate MEP which leads from S_1 diazirine to S_1 diazomethane. Then, we have used the program previously written by ourselves^{24b} to project out of the Hessian matrix the zero-frequency modes in a conical intersection. In this case, only seven directions are projected out of \mathbf{H} : the energy gradient plus the six translation and rotation modes. The structure of the bifurcation along with its featuring eigenvector is shown in Figure 3d.

Second- and Third-Excited-State Potential Energy Surfaces. In the observed strong absorption region of diazirine at 200 nm (6.20 eV),³⁹ we found a saddle point with C_{2v} symmetry corresponding to a $\pi-\pi^*$ (B_2) excitation, $\lambda_{00} = 207$ nm (Figure 4a). Above this surface, there is a third excited state with $\sigma-\pi^*$ (A_2) character, $\lambda_{00} = 200$ nm. The stationary point that is found on the A_2 surface (Figure 4b) is a minimum; all of the frequencies are real.

Above the first excited state of diazomethane, there are three other valence excited states, yielding the corresponding stationary geometries in C_{2v} symmetry (Table 1). These structures are not minima but are saddle points on the respective surfaces. The normal modes associated with each of the imaginary frequencies of such points are represented in Figure 4c–e.

The S_2 excited states of diazirine (B_2) and diazomethane ($2A_1$) are again connected along a C_s reaction coordinate. The ring opening of the S_2 cyclic structure leads to a transition state (TS2, Figure 4f), 30 kcal/mol above the B_2 state of diazirine. Deformation of the molecular structure of TS2 in the forward direction of its transition vector, as plotted in Figure 4f, ends at an S_2/S_1 conical intersection (CI2, Figure 4g). On the other hand, motion along the normal mode of imaginary frequency of $2A_1$ diazomethane leads to the same S_2/S_1 conical point.

Dynamic Simulation of Methylene Formation. In this section, we present the direct ab initio semiclassical trajectories propagated on the fly onto the S_1 and S_0 surfaces. Provided that CASSCF is still an expensive method to carry out this kind of computations, only a very small region of the phase space has been sampled, so our calculations lack of statistical meaning. However, very important mechanistic conclusions arise from them.

As pointed out in the preceding sections, S_1 diazomethane has a C_{2v} stationary geometry which is not a minimum but a first-order saddle point on the S_1 surface. Furthermore, it was demonstrated that there is a very well-defined path leading from S_1 diazomethane to an S_1/S_0 conical intersection where a very efficient radiationless deactivation of S_1 takes place. Thus, if the system evolves in such a way that passes exactly through the conical point, then it should follow the steepest descent slope⁴⁰ of the S_0 surface, that is, the direction of maximum gradient difference, regenerating S_0 diazomethane. Moreover, in the case that the jump from the upper to the lower state occurs at a point which is only near the surface crossing (a necessary condition to have a finite probability of hopping), an amount of energy equal to the height of the jump is converted into a component of the momentum directed along the nonadiabatic coupling vector, which is, of course, superimposed on the nuclear momentum before the jump. Thus, dynamic trajectory calculations become very useful tools to elucidate the evolution of the system after the surface hop.

Several trajectories were started at the S_1 diazomethane transition state by adding translational energy along some selected directions corresponding to excited normal modes of diazomethane; no rotational energy was added in any case.

Figures 5 and 6 illustrate the formation of carbene in its lowest singlet state after radiationless deactivation of the precursor, S_1 diazomethane. The second and third excited modes, in increasing frequency order, were sampled with 5.0 kcal/mol, respectively, plus 0.1 kcal/mol along the transition mode in each case. These motions correspond to out-of-plane vibrations being “parallel” to the nonadiabatic coupling vector at the surface crossing point. They are the only modes able to induce an effective surface hop.

A. Sampling of Mode 2. The most important motions at the beginning of the trajectory (0–50 fs) are (1) torsion (Γ_{HCHN})

(37) Castaño, O.; Frutos, L.-M.; Palmeiro, R.; Notario, R.; Andrés, J. L.; Gomperts, R.; Blancafort, L.; Robb, M. A. *Angew. Chem., Int. Ed.* **2000**, *39*, 2095.

(38) (a) Basilevsky, M. V. *Chem. Phys.* **1977**, *24*, 81. (b) Valtzanos, P.; Ruedenberg, K. *Theor. Chem. Acta* **1986**, *69*, 281.

(39) Hoffmann, R. *Tetrahedron* **1966**, *23*, 539.

(40) Klessinger, M.; Michl, J. *Excited States and Photochemistry of Organic Molecules*; WCH Publishers: New York, 1995.

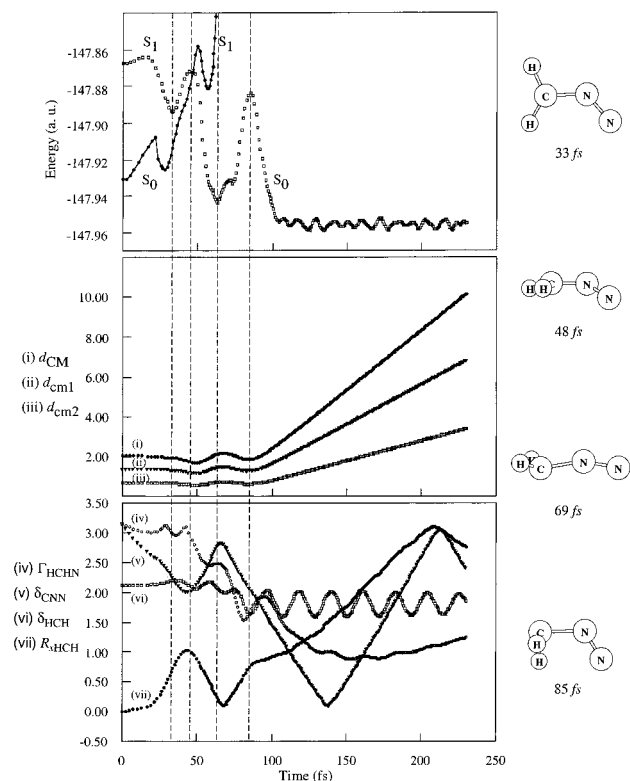


Figure 5. (a) Energy profiles of the S_1 and S_0 states as time functions. (b) Distance between the mass centers of (i) CH_2 and N_2 fragments, (ii) CH_2 and whole molecule, and (iii) N_2 and whole molecule. (c) Time evolution of (iv) torsion Γ_{HCHN} , (v) out-of-plane bending δ_{CNN} , (vi) CH_2 bending δ_{HCH} , and (vii) rotation of the CH_2 fragment around its x -axis.

and (2) out-of-plane bending (δ_{CNN}), which are in turn the main internal coordinates defining mode 2, being, of course, superimposed on the in-plane bend coordinate (δ'_{CNN}), the imaginary frequency mode. These deformations increase until they reach their respective local maximum displacements, which occurs at 48 fs, concurrent with surface hopping. After the hop, the system executes a single vibrational period localized in one coordinate (CN stretching). Then, part of the energy is transferred to CN elongation (85 fs), which causes dissociation of the molecule into two fragments with almost half of the initial energy released in translational form (4000 m/s CH_2 , 2000 m/s N_2). In the right-hand side of Figure 5, the molecular rearrangements corresponding to some featuring points are shown. For example, (i) the rather nonplanar structure of the hop is localized at a point which is 15 kcal/mol above the lowest energy point of the $(3N - 8)$ -dimensional conical intersection and (ii) the molecular geometry at 85 fs is very close to the transition state found on the S_0 surface of 3H-diazirine leading to the dissociation products (TS1, Figure 2b).

B. Sampling of Mode 3. The energy profiles of S_1 and S_0 states along this trajectory are represented in Figure 6a. The distortions of the molecular geometry, as a time function, are collected in Figure 6b,c. This trajectory follows the same pattern as sampling of mode 2: the surface hop takes place quite early along the molecular travelling on the potential surface (39 fs; 11 kcal/mol above the lowest energy point of the S_1/S_0 CI1 conical intersection), and then the region of S_0 diazomethane minimum is reached. The excess of energy, resulting from electronic deexcitation, flows into CN stretching which leads

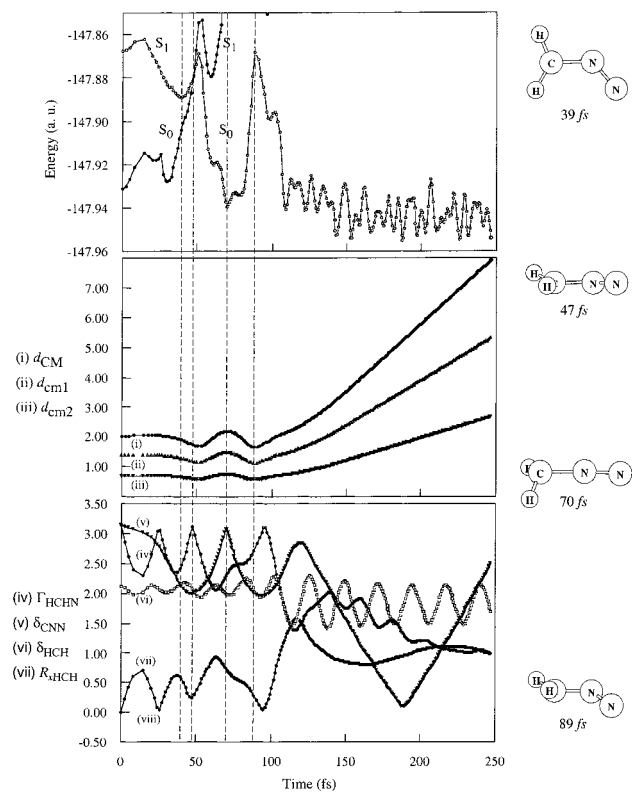


Figure 6. (a) Energy profiles of S_1 and S_0 states as time functions. (b) Distance between the mass centers of (i) CH_2 and N_2 fragments, (ii) CH_2 and whole molecule, and (iii) N_2 and whole molecule. (c) Time evolution of (iv) torsion Γ_{HCHN} , (v) out-of-plane bending δ_{CNN} , (vi) CH_2 bending δ_{HCH} , and (vii) rotation of the CH_2 fragment around its x -axis.

to dissociation of the molecule after passing near the TS1 structure (89 fs). The velocities of the fragments are 2900 and 1450 m/s, for CH_2 and N_2 , respectively.

C. Dynamics on the Second Excited State. Figure 7 illustrates the trajectory run starting at the Franck–Condon region of S_0 diazomethane on the S_2 surface. No energy is added to any vibrational mode. The system directly decays onto the S_2/S_1 conical intersection region (CI2, Figure 4g) by activation of the CNN out-of-plane bending coordinate. However, the molecule hops the third time that S_2 and S_1 surfaces touch each other (40 fs; 12 kcal/mol above the lowest energy point of the S_2/S_1 CI2 conical intersection). After the hop, the C–N internuclear distance (Figure 7b) starts to increase which leads to dissociation of the molecule into methylene and molecular nitrogen. In principle, this bond breaking would produce excited carbene; however, the flow of the energy into δ_{HCH} causes deactivation of methylene through an S_1/S_0 conical intersection, yielding carbene in its lower singlet state. For more complex carbenes, which lack this internal motion or are hindered, this route could generate the excited species. It is worthwhile noting that the velocities of the resulting fragments are much higher than those arising from excitation into the S_1 surface (6300 m/s CH_2 , 3150 m/s N_2).

Conclusions

The processes involved in the photochemistry of the parents of the diazirine and diazo families (Figure 8) have been studied at the CASSCF (12e, 10o) + CASPT2 levels in conjunction with a quite high quality basis set (cc-pVTZ).

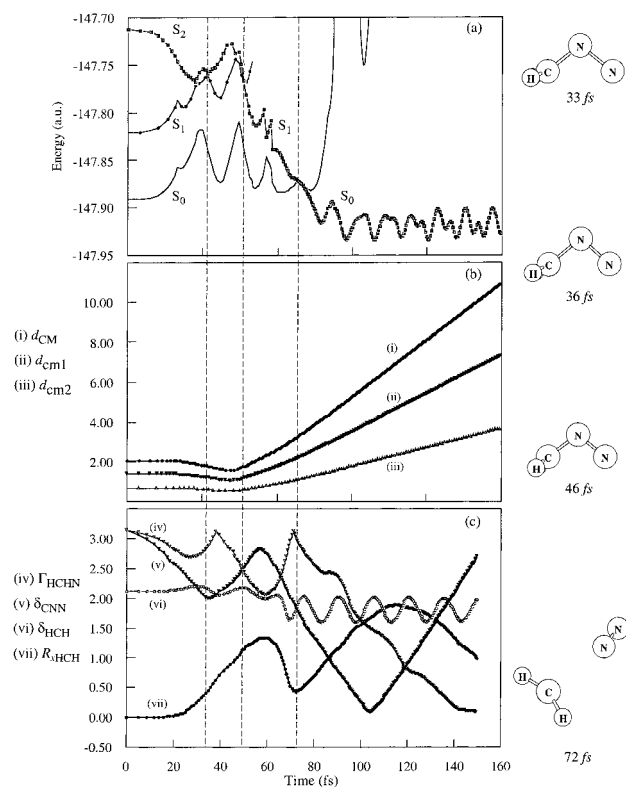


Figure 7. (a) Energy profiles of the S_2 , S_1 , and S_0 states as time functions. (b) Distance between the mass centers of (i) CH_2 and N_2 fragments, (ii) CH_2 and whole molecule, and (iii) N_2 and whole molecule. (c) Time evolution of (iv) torsion Γ_{HCHN} , (v) out-of-plane bending δ_{CNN} , (vi) CH_2 bending δ_{HCH} , and (vii) rotation of the CH_2 fragment around its x -axis.

On the S_0 surface, we found only two transition states: the first connects diazirine with diazomethane while the second connects diazirine with the dissociation products. We do not expect a transition state leading from diazomethane to nitrogen extrusion because the only channel to be exploited is that which passes through a bending in plane structure, but this corresponds to an S_1/S_0 conical intersection (CI1, Figure 3c). Consequently, the system should avoid this path when it is in the ground state.

On the S_1 surface, in accordance with the CIS calculations of Platz and co-workers,^{7f} we found no minimum for diazirine; the only stationary structure found on this region is a first-order saddle point. Furthermore, the same situation applies to diazomethane. Therefore, there are two transition states connected along a C_s reaction coordinate, which is mainly localized in the CNN out-of-plane deformation. Moreover, it is unlikely that S_1 diazirine isomerizes to S_1 diazomethane following this path, because vibrational coupling to other modes will part the system from the isomerization route. In any case, this question is irrelevant, provided that, whether isomerization takes place or not, trajectories starting at each of these transition geometries will evolve to a common locus on the potential energy surface: the S_1/S_0 conical intersection, where a very efficient nonradiative deexcitation occurs. Afterward, the system has enough internal energy to surmount the barrier that leads to the dissociation products in the S_0 state. Therefore, our calculations support the hypothesis of Moore and Pimentel⁵ that diazomethane is generated in the photolysis of diazirine by recombination of the two fragments methylene and nitrogen. This is as well in accordance with photolysis in solution of either diazirine or diazomethane, which gives methylene with equal yields.⁴¹

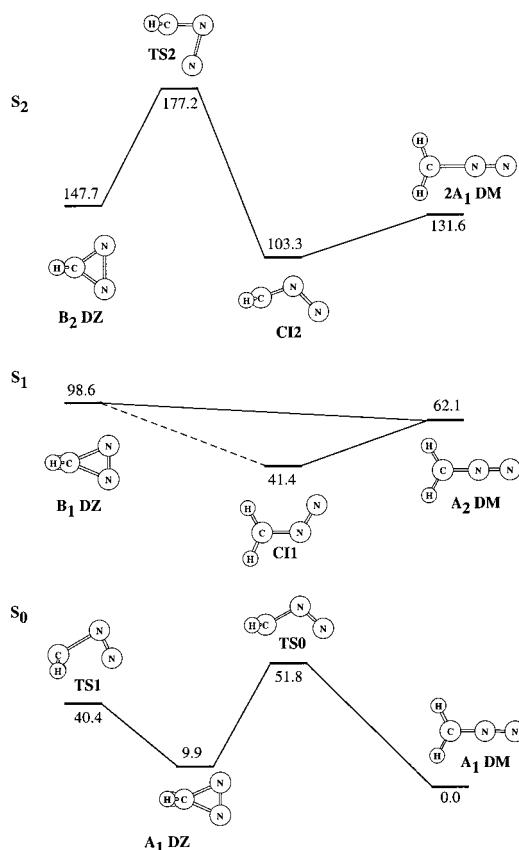


Figure 8. Schematic representation of the most relevant reaction steps involved in the photochemistry of 3H-diazirine and diazomethane. Relative energies including zero point corrections are given in kcal/mol.

The topology of the S_2 surface is somewhat different from that of the lower S_1 state. The stationary structures corresponding to both isomers are first-order saddle points. Both geometries are again connected along a C_s reaction coordinate, and there are a transition state (TS_2 , Figure 4f) and an S_2/S_1 conical intersection (CI_2 , Figure 4g) between them. We have demonstrated that trajectories passing through this conical intersection cause dissociation of the molecule into singlet carbene and molecular nitrogen. Therefore, diazirine–diazo isomerization cannot take place on the S_2 surface. It is clear that formation of excited carbene will be more effective if diazomethane is the starting material instead of diazirine, because the latter needs to surmount a quite large energy barrier before reaching the conical intersection region.

To finish, the mechanism proposed for carbene generation differs completely from that of ref 12, where it was postulated that carbene formation proceeded through a second S_1/S_0 conical intersection, which, in our opinion, is an artifact of the calculations. We demonstrate in this work by means of dynamical calculations that no carbene formation takes place in the excited state; it is formed on the ground-state surface after decaying through a conical intersection (CI_1), while this decaying path was taken instead to lead to diazomethane formation in ref 12. Furthermore, starting at the second excited state, we arrive as well at carbene formation in the ground state (this possibility is not explored in refs 11 and 12). Therefore, irrespective of which particular surface is populated, we always

(41) Turro, N. J.; Cha, Y.; Gould, I. R. *J. Am. Chem. Soc.* **1987**, *109*, 2101.

get the same final product. This is in contradiction with ref 12, where wavelength dependence is proposed for generation of carbene or diazomethane. It must be pointed out that the observed differences between the mechanisms proposed in both works (ref 12 and the present one) come from the choice of the active space. On the other hand, the minimal active space required to treat this kind of systems is eight electrons distributed in seven orbitals, at least for the region of the potential energy surface dominated by diazomethane rearrangement.

Acknowledgment. This research has been supported by the Ministerio de Ciencia y Tecnología of Spain under Project No. BQU2000-1353. The authors thank D. R. Larrosa for technical support in running the calculations and SCAI (University of Málaga) for the use of an Origin 2000 SGI computer. This work is dedicated to the memory of the late Prof. Juan I. Marcos.

Supporting Information Available: Figures of IRC calculations mentioned in the text at the CASSCF(8e,8o)/6-31G* level. Figures of normal modes for S_0 and S_1 diazomethane at the CASSCF(12e,10o)/cc-pVTZ level. Tables containing CASSCF(12e,10o)/cc-pVTZ-optimized Cartesian coordinates, absolute total energy values (hartrees) at the CASPT2(12e,10o) level, and CASSCF(12e,10o)/cc-pVTZ harmonic frequencies for the all the structures mentioned in Table 2. Two tables comparing geometrical parameters, relative energies, and harmonic frequencies calculated with two different active spaces [(12e, 10o); (8e, 7o)] and two different basis sets (cc-pVTZ; 6-31G*), respectively, for S_0 and S_1 diazomethane. (PDF) This material is available free of charge via the Internet at <http://pubs.acs.org>.

JA010750O